

This project has received funding from the European Community's Horizon 2020 Framework Programme under grant agreement 820774

**MANUELA**  
Additive Manufacturing  
using Metal Pilot Line

## Deliverable D4.3

### Development and calibration of the on-line process monitoring for material of interest (1)

#### WP 4

<b>Deliverable Status</b>	<b>DRAFT</b>
<b>Type</b>	<b>REPORT</b>
<b>Dissemination level (according to the proposal)</b>	<b>PUBLIC</b>

Project Name:	MANUELA - Additive Manufacturing using Metal Pilot Line
Grant Agreement:	820774
Project Duration:	1 October 2018 – 30 September 2022

## Document Information

Work package	WP4
Lead beneficiary	FAU

Due Date	12/31/2019	Due date in months	15
Date of submission	12/27/2019	Month of submission	15

Status	Authors name and Company/Organisation	Date
Prepared by	Daniel Gage / Friedrich-Alexander University	12/10/2019
Reviewed by	Lars Nyborg, Chalmers	12/27/2019
	Eduard Hryha, Chalmers	12/27/2019
Approved by	Lars Nyborg, Chalmers	12/27/2019

## Contents

<b>Executive Summary</b> .....	<b>3</b>
<b>1 Introduction</b> .....	<b>4</b>
<b>2 Defect detection</b> .....	<b>5</b>
2.1 Detection of Pores .....	6
2.2 Detection of uneven surfaces .....	7
2.3 Defects regarding the dimensional accuracy .....	7

<b>3</b>	<b>Increasing the process robustness and repeatability</b> .....	<b>7</b>
<b>4</b>	<b>ELO scan parameters</b> .....	<b>8</b>
<b>5</b>	<b>Conclusion</b> .....	<b>11</b>
<b>6</b>	<b>Literaturverzeichnis</b> .....	<b>12</b>

## List of Figures

Figure 1: Schematic of the EBM process cycle. [1] .....	4
Figure 2: Occurring defects in samples built using the EBM process. a: Images of the top surfaces of a porous, a good and an uneven sample. b: Image of a cross section of an uneven sample. [2] .....	5
Figure 3: Test sample for the EBM process with implemented on-line monitoring using the ELO system. Right: Cross section of the test sample. ....	5
Figure 4: BSE Intensity distribution in dependence of the angle of incidence. [3] .....	6
Figure 5: Schematic of the electron backscattering influenced by a pore. [3, 4].....	6
Figure 6: ELO image of a dense (left) and a porous (right) test sample. Resolution: 1500 x 1500 pixels. Exposure time per pixel: 0.4 $\mu$ s. Pixel size: 60 $\mu$ m. ....	6
Figure 7: Schematic of the electron backscattering influenced by an uneven surface. [3, 4]..	7
Figure 8: ELO image of a dense (left) and an uneven (right) test sample. Resolution: 2500 x 2500 pixels. Exposure time per pixel: 0.4 $\mu$ s. Pixel size: 36 $\mu$ m. ....	7
Figure 9: ELO images of the same layer with different beam currents during the ELO scans. Resolution: 1500 x 1500 pixels. Exposure time per pixel: 0.4 $\mu$ s. Pixel size: 60 $\mu$ m. ....	9
Figure 10: ELO images of the same layer with different scan and pixel sizes. Resolution: 1500 x 1500 pixels. Exposure time per pixel: 0.4 $\mu$ s. ....	9
Figure 11: ELO images of the same layer with different pixel resolutions and pixel sizes. Exposure time per pixel: 0.4 $\mu$ s. ....	10

## Terms and definitions

<b>Acronym</b>	<b>Description</b>
<b>AM</b>	Additive Manufacturing
<b>LPBF</b>	Laser power bed fusion
<b>EBM</b>	Electron beam melting
<b>ELO</b>	Electron optical
<b>SEM</b>	Scanning electron microscope
<b>BSE</b>	Backscattered electron(s)
<b>CT</b>	Computer tomography
<b>KPI</b>	Key performance indicator
<b>FAU</b>	Friedrich-Alexander Universität Erlangen-Nürnberg, Germany

## Executive Summary

By using new on-line monitoring systems, the MANUELA pilot line will improve metal AM. For the EBM process, the ELO system monitors each layer using a detector for backscattered electrons. The report D4.6 'Online monitoring systems calibrated and tested' provides more information about the on-line monitoring of the LPBF process.

The outcome of on-line monitoring using the ELO system provides in-situ defect detection of pores, uneven surfaces and poor dimensional accuracy.

# 1 Introduction

The MANUELA pilot line will implement on-line monitoring during powder bed based AM. This will increase the process robustness and support the process development. The on-line monitoring will enable a high-level quality control of the products as well.

This report comprises the on-line monitoring during the EBM process. The on-line monitoring of the LPBF process is described in the report D4.6 'Online monitoring systems calibrated and tested'.

For the EBM process, FAU uses a retrofitted Arcam S12, namely the "ATHENE". In this EBM machine a so called Electron Optical (ELO) system generates images of the current layer using backscattered electrons (BSE). For image generation, the electron beam scans the current layer with low beam current. Meanwhile the BSE detector measures the signal. Therefore, the image generation procedure is similar to a scanning electron microscope (SEM) in its BSE mode.

Figure 1 shows the state of the art EBM process cycle. After applying a new powder layer, the electron beam heats up the powder, before melting it. Afterwards, lowering the platform enables the next application of powder. The layerwise image generation is a novel process step in the EBM process cycle placed between the Melting and the Lowering of the platform.

The new process step allows detecting defects during any build job.

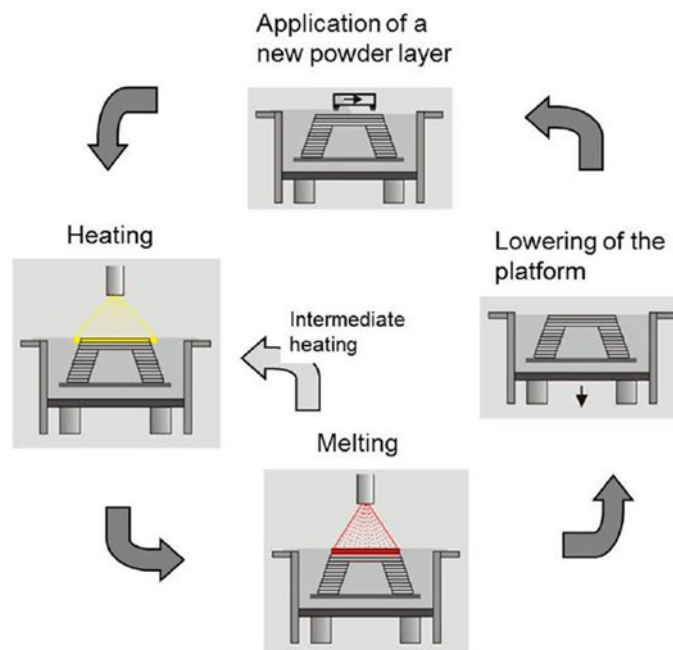


Figure 1: Schematic of the EBM process cycle. [1]

## 2 Defect detection

Two main defects, occurring in EBM processed parts, are pores and uneven surfaces. Figure 2 shows the top surfaces of a porous, a good and an uneven sample. Additionally, it shows a cross section of an uneven sample. Pores are detrimental for the mechanical properties. Uneven surfaces lead to poor dimensional accuracy regarding the top surface of the sample. Furthermore, the application of a new powder layer requires an even surface. Therefore, uneven surfaces can lead to process abortion.

The greyscale ELO image contains information about the local BSE signal in the form of brightness of pixels. Understanding the physical background of electron backscattering is essential to interpret ELO images correctly and thereby essential for defect detection.

This report will present the usage of the ELO system during building the sample shown in Figure 3.

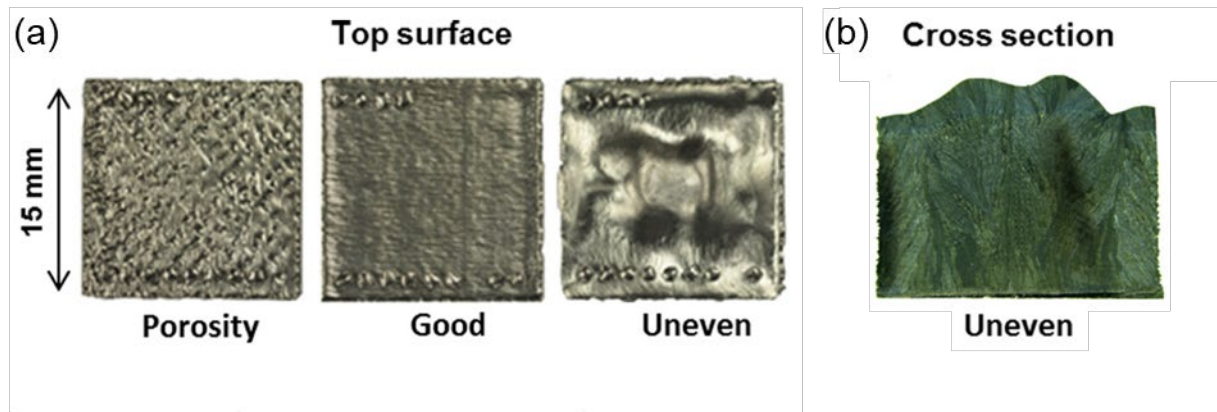


Figure 2: Occurring defects in samples built using the EBM process. a: Images of the top surfaces of a porous, a good and an uneven sample. b: Image of a cross section of an uneven sample. [2]

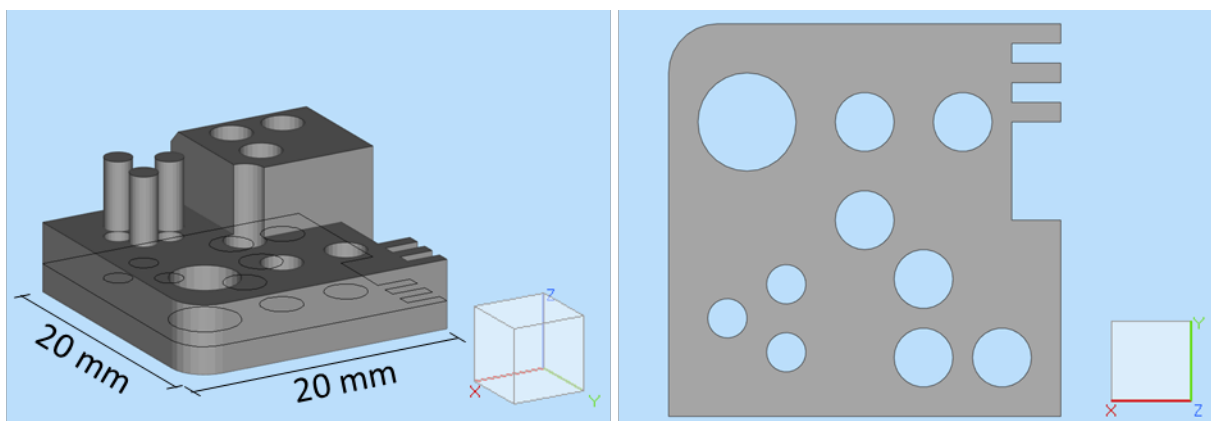


Figure 3: Test sample for the EBM process with implemented on-line monitoring using the ELO system. Right: Cross section of the test sample.

## 2.1 Detection of Pores

Figure 4 shows the BSE intensity in dependence of the angle of incidence. With an increasing angle, the intensity directed to the electron source decreases. Therefore, the amount of electrons hitting the BSE detector decreases as well due to its position in the "ATHENE". Including this correlation between the angle of incidence and the BSE intensity, Figure 5 shows a schematic of the multiple electron backscattering resulting from scanning a pore. Consequently, scanning a pore leads to a decreased amount of electrons hitting the BSE detector in comparison to a flat and dense surface. Therefore, the ELO image shows a dark pixel. Figure 6 presents ELO images of a dense and a porous test sample. Furthermore, Figure 6 demonstrates the applicability of the ELO system for pore detection.

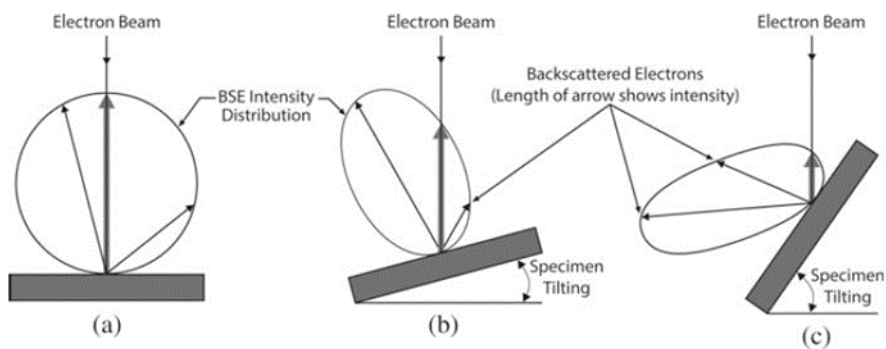


Figure 4: BSE Intensity distribution in dependence of the angle of incidence. [3]



Figure 5: Schematic of the electron backscattering influenced by a pore. [3, 4]

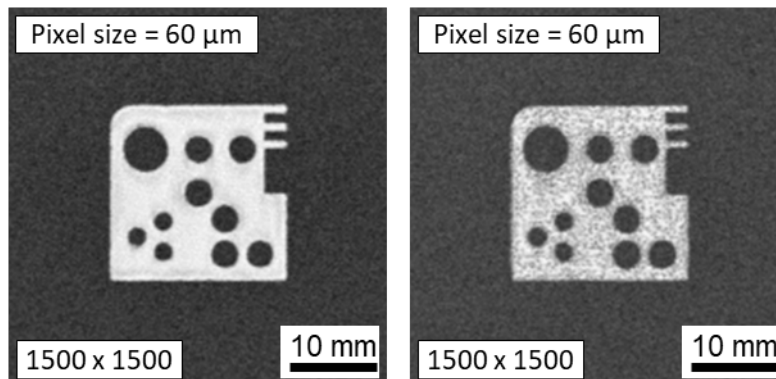


Figure 6: ELO image of a dense (left) and a porous (right) test sample. Resolution: 1500 x 1500 pixels. Exposure time per pixel: 0.4  $\mu$ s. Pixel size: 60  $\mu$ m.

## 2.2 Detection of uneven surfaces

Figure 7 provides a schematic of the electron backscattering while scanning an uneven surface. The schematic is based on the correlation between the BSE intensity and the angle of incidence, shown in Figure 4. Compared to a flat and dense surface the amount of electrons reaching the BSE detector is less. However, more electrons hit the detector scanning an uneven surface than scanning a pore. Figure 8 shows ELO images of a dense and an uneven test sample. This demonstrates that the ELO observation is able to detect uneven surfaces.

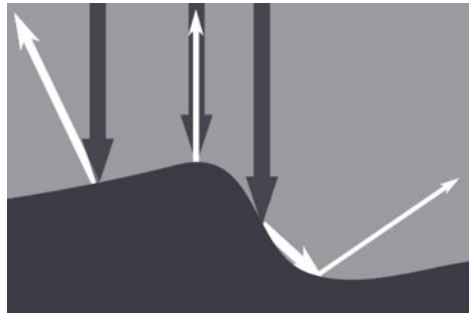


Figure 7: Schematic of the electron backscattering influenced by an uneven surface. [3, 4]

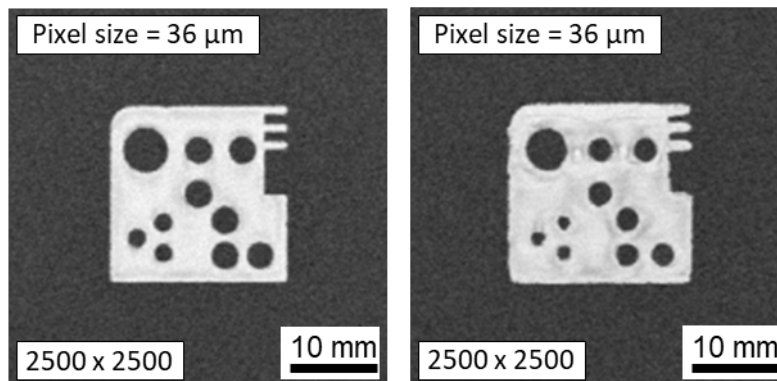


Figure 8: ELO image of a dense (left) and an uneven (right) test sample. Resolution: 2500 x 2500 pixels. Exposure time per pixel: 0.4  $\mu$ s. Pixel size: 36  $\mu$ m.

## 2.3 Defects regarding the dimensional accuracy

Figure 8 shows ELO images of a dense and an uneven sample. The contours of both samples and the three pins on the top right corner differ. Comparing the CAD cross section of the test sample, shown in Figure 3, with these ELO images demonstrates the dimensional accuracy of the built samples, which is poor for the uneven sample and good for the dense sample.

Therefore, the implementation of the ELO observation enables an in-situ inspection of the dimensional accuracy, due to the high contrast between the powder bed and the molten surface.

## 3 Increasing the process robustness and repeatability

If defects occur, an adjustment of the process parameters will be necessary. Conventionally, this results in an additional build job using the adjusted parameters. However, the on-line

monitoring enables an in-situ adjustment based on detected defects. Strategies for such adjustments will be developed.

The detection of defects and especially in-situ parameter adjustment lead to an increased process robustness.

Additionally, the in-situ defect detection and parameter adjustment accelerate the process development by reducing the effort of analysing shifts of the processing window. Such shifts can occur building challenging geometries.

Furthermore, the on-line monitoring using the ELO system generates a large amount of data. This data can be used to enlarge the knowledge about process variations and improve the robustness and repeatability of AM by adapting the process windows.

## 4 ELO scan parameters

The ELO scan offers four adjustable parameters:

- Beam current
- Size of the scanned area
- Resolution in pixels
- Exposure time per pixel

Figure 9 shows ELO images generated using different beam currents. All images show the same layer. The quality of the ELO image depends on the ratio of the usable BSE signal to the noise. The image generated with a beam current of 0.5 mA is almost blurry. Using a beam current of 15 mA provides a good ELO image. However, using high beam currents can result in melting the scan area. The standard beam current for the ELO scan of 3 mA provides good images and avoids high risk of melting the scan area.

Figure 10 presents ELO images with different scan sizes but equal pixel resolutions. With a small scan size and a high pixel resolution, the spatial resolution increases. However, the highest achievable spatial resolution depends on the beam diameter [3], which amounts to about 400  $\mu\text{m}$ . Nevertheless, the scan size will always be adjusted to the part size.

Figure 11 shows ELO images with different pixel resolutions of the same layer. The image with a resolution of 100 x 100 pixels is blurry. With increasing pixel resolution, the image quality increases, of course. However, this leads to an increased duration of the ELO scan as well. Taking into account, that the typical layer thickness for the EBM process is 50  $\mu\text{m}$ , the usage of higher resolution can lead to a significant increase of the total process duration.

Consequently, depending on the on-line monitoring requirements the ELO scan will be adjusted for every part.

This project has received funding from the European Community's Horizon 2020 Framework Programme under grant agreement 820774

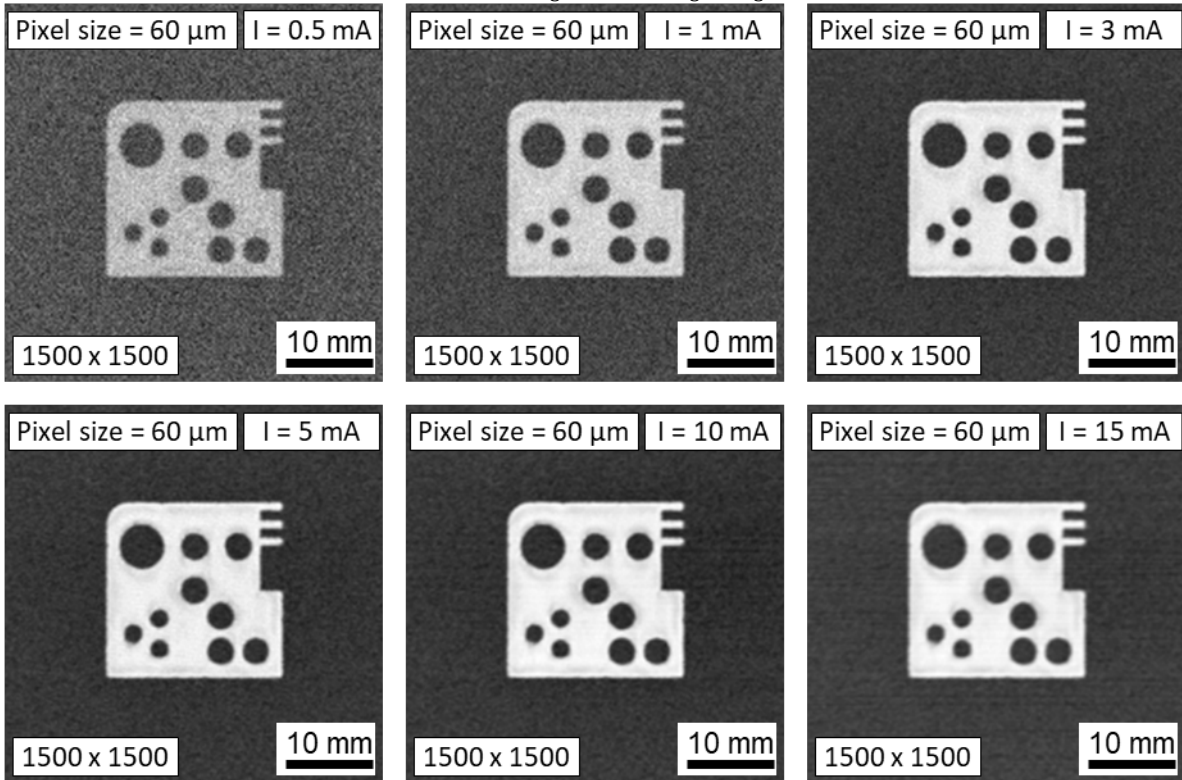


Figure 9: ELO images of the same layer with different beam currents during the ELO scans. Resolution: 1500 x 1500 pixels. Exposure time per pixel: 0.4  $\mu$ s. Pixel size: 60  $\mu$ m.

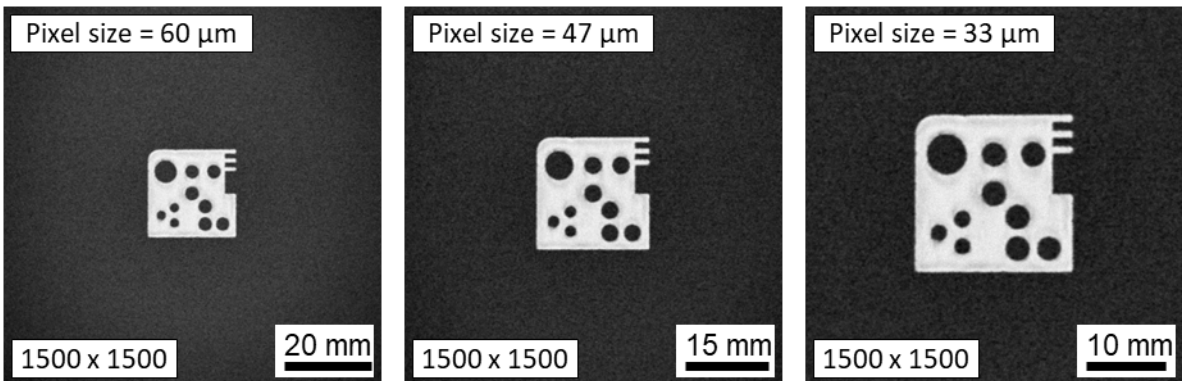


Figure 10: ELO images of the same layer with different scan and pixel sizes. Resolution: 1500 x 1500 pixels. Exposure time per pixel: 0.4  $\mu$ s.

This project has received funding from the European Community's Horizon 2020 Framework Programme under grant agreement 820774

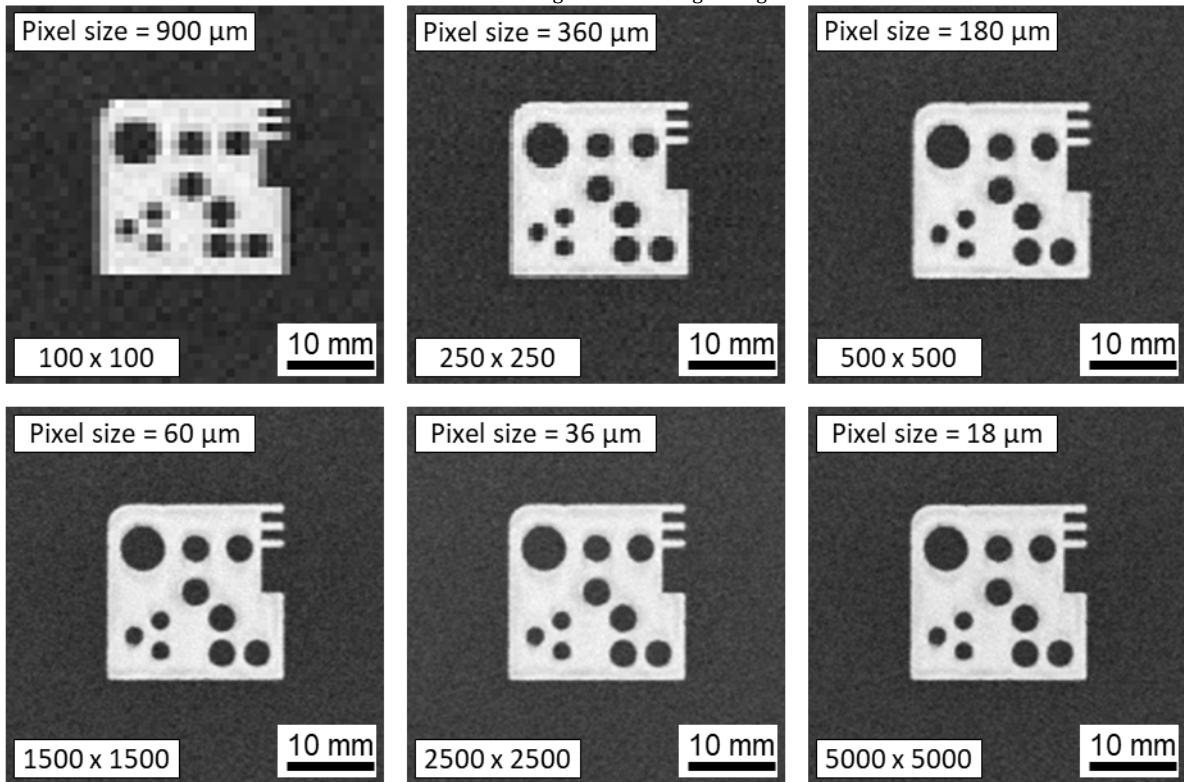


Figure 11: ELO images of the same layer with different pixel resolutions and pixel sizes. Exposure time per pixel: 0.4  $\mu\text{s}$ .

## 5 Conclusions

This report shows the excellent applicability of the ELO system for EBM on-line monitoring. The ELO system provides qualitative information about pores, uneven surfaces and the dimensional accuracy. Future investigations will check if quantitative on-line monitoring is applicable as well.

The current state of the ELO system already provides an increased process robustness and supports the process development. Due to further ELO observation development, the correlation of the ELO observation with the process development will become more distinct.

For high quality on-line monitoring, the resolution should be as high as possible. However, with improved resolution the ELO scan duration increases. Therefore, MANUELA pilot line customers can choose different on-line monitoring quality levels resulting in different manufacturing durations.

In April 2021, a 2<sup>nd</sup> report about the on-line monitoring will provide further development.

## 6 Literature

- [1] KÖRNER, C.: *Additive manufacturing of metallic components by selective electron beam melting — a review*. In: *International Materials Reviews* 61 (2016), Nr. 5, S. 361–377
- [2] JUECHTER, V. ; SCHAROWSKY, T. ; SINGER, R. F. ; KÖRNER, C.: *Processing window and evaporation phenomena for Ti–6Al–4V produced by selective electron beam melting*. In: *Acta Materialia* 76 (2014), S. 252–258
- [3] UL-HAMID, Anwar: *A Beginners' Guide to Scanning Electron Microscopy*. Cham : Springer International Publishing, 2018
- [4] JONAS BÖHM: *Untersuchung des Rückstreuelektronensignals bei der Erzeugung von Schmelzflächen mit dem Elektronenstrahl*. Friedrich Alexander Universität Erlangen-Nürnberg, WTM. Bachelorarbeit. 2019